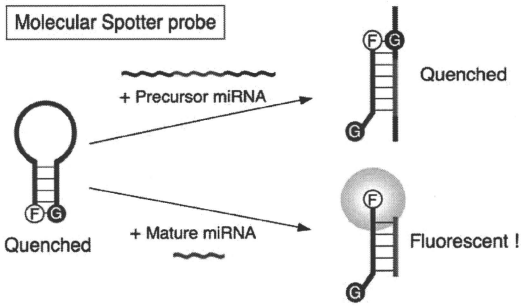

Fig. 1. Schematic representation of molecular spotter probe. One end of the probe is cytosine covalently linked with a fluorophore BODIPY-FL (F), which is quenched by the adjacent guanine base (G) through the base-pairing. The probe is designed to be quenched due to the guanine base in the precursor RNA. Only when the mature RNA is hybridized, the probe emits fluorescence.

DISCUSSION. The molecular spotter probe can hybridize to both the mature and precursor miRNA sequences; the fluorophore of the probe by itself is quenched by its complementary pairing to the guanine base. Hence, the elimination of the probe
from the sample solution is not needed for the specific detection of target RNA. In comparison with the molecular beacon, since the natural guanine base is the quencher of BODIPY-FL fluorophore, the additional quencher molecules such as Dabcyl are not necessary. Direct fluorescence detection without any enzymatic reactions allows real-time quantitative monitoring of the target RNAs.

ACKNOWLEDGEMENT. This work is supported by KAKENHI.

REFERENCES.

1. Tyagi, S., and Kramer, F.R. (1996) Nat. Biotechnol. 14, 303-308
2. Kurata, S., Kanagawa, T., Yamada, K., Torimura, M., Yokomaku,T., Kamagata, Y., and Kurane, R. (2001) Nucleic Acids Res. 29, e34

Developmental Cell
Article

A Systems Approach Reveals that the Myogenesis Genome Network Is Regulated by the Transcriptional Repressor RP58

Shigetoshi Yokoyama,[1,7] Yoshiaki Ito,[1,7] Hiroe Ueno-Kudoh,[1] Hirohito Shimizu,[1] Kenta Uchibe,[1] Sonia Albini,[2] Kazuhiko Mitsuoka,[1] Shigeru Miyaki,[1] Minako Kiso,[1] Akane Nagai,[1] Tomohiro Hikata,[1] Tadahiro Osada,[1] Noritsugu Fukuda,[1] Satoshi Yamashita,[1] Daisuke Harada,[1] Valeria Mezzano,[2] Masataka Kasai,[3] Pier Lorenzo Puri,[2,4] Yoshihide Hayashizaki,[5] Haruo Okado,[6] Megumi Hashimoto,[1] and Hiroshi Asahara[1,*]

[1]Department of Systems BioMedicine, National Research Institute for Child Health and Development, Setagaya, Tokyo 157-8535, Japan
[2]The Burnham Institute for Medical Research, La Jolla, CA 92037, USA
[3]Department of Immunology, National Institute of Infectious Diseases, Shinjuku, Tokyo 162-8640, Japan
[4]Dulbecco Telethon Institute, IRCCS Santa Lucia Fondation and European Brain Research Institute (EBRI), 64 Via del Fosso di Fiorano, 00143 Rome, Italy
[5]Laboratory of Genome Exploration Research Group, RIKEN Genomic Sciences Center (GSC), RIKEN Yokohama Institute, Yokohama, Kanagawa 230-0045, Japan
[6]Department of Molecular Physiology, Tokyo Metropolitan Institute for Neuroscience, Fuchu, Tokyo 183-8526, Japan
[7]These authors contributed equally to this work
*Correspondence: asahara@nch.go.jp
DOI 10.1016/j.devcel.2009.10.011

SUMMARY

We created a whole-mount in situ hybridization (WISH) database, termed EMBRYS, containing expression data of 1520 transcription factors and cofactors expressed in E9.5, E10.5, and E11.5 mouse embryos—a highly dynamic stage of skeletal myogenesis. This approach implicated 43 genes in regulation of embryonic myogenesis, including a transcriptional repressor, the zinc-finger protein *RP58* (also known as *Zfp238*). Knockout and knockdown approaches confirmed an essential role for *RP58* in skeletal myogenesis. Cell-based high-throughput transfection screening revealed that RP58 is a direct MyoD target. Microarray analysis identified two inhibitors of skeletal myogenesis, *Id2* and *Id3*, as targets for RP58-mediated repression. Consistently, MyoD-dependent activation of the myogenic program is impaired in *RP58* null fibroblasts and downregulation of *Id2* and *Id3* rescues MyoD's ability to promote myogenesis in these cells. Our combined, multisystem approach reveals a MyoD-activated regulatory loop relying on RP58-mediated repression of muscle regulatory factor (MRF) inhibitors.

INTRODUCTION

Spatiotemporal expression of transcription factors (TFs) plays a central role in cell differentiation and organ development during embryogenesis (Burke et al., 1995; Gray et al., 2004; Jessell, 2000). Combinatorial activity of TFs positively or negatively regulates specific gene expression patterns essential for tissue development and cell fate determination.

Skeletal myogenesis, in which myogenic precursors differentiate into myoblasts and then form multinucleated myotubes, is an ideal system to understand multistaged transcriptional regulatory networks functioning during vertebrate development (Arnold and Braun, 1996). During skeletal myogenesis, distinct subsets of genes are expressed with partially overlapping kinetics to form a complex network of interdependent pathways (Blais et al., 2005; Cao et al., 2006; Penn et al., 2004). The muscle-specific basic helix-loop-helix (bHLH) transcription factors, MyoD, Myf5, Myogenin (Myog), and MRF4, initiate and perpetuate the myogenic program in collaboration with MEF2. Genetic evidence indicates that MyoD and/or Myf5 are critical for myogenic cell fate (Braun et al., 1992; Rudnicki et al., 1992), whereas Myog regulates terminal differentiation (Hasty et al., 1993; Nabeshima et al., 1993). MRF4 is suggested to act at both early determination and terminal differentiation stages (Kassar-Duchossoy et al., 2004; Zhang et al., 1995). Muscle bHLH proteins bind the E-box sequence (CANNTG) on regulatory elements of muscle genes, often in close proximity with MEF2 binding sites (Puri and Sartorelli, 2000). Heterodimerization of bHLH proteins with E-proteins (E12/E47) allows productive interaction with the E-box (Blackwell et al., 1990; Blackwell and Weintraub, 1990; Murre et al., 1989) and is regulated indirectly by Id proteins, which are HLH transcription factors lacking DNA-binding basic domains (Benezra et al., 1990). These proteins sequester E-proteins into inactive complexes, thereby preventing formation of bHLH/E-proteins heterodimers and their DNA-binding and transcriptional activities. Consistent with a proposed role for Id proteins as inhibitors of terminal differentiation, *Id* mRNAs are detected in proliferating skeletal muscle and are downregulated in differentiated muscle cultures (Benezra et al., 1990; Chen et al., 1997).

Recent genome-wide approaches using chromatin immunoprecipitation (ChIP) to assess binding activity of MyoD and Myog to a promoter array reveal a complex mechanism coordinating expression of distinct subsets of genes by these critical activators during skeletal myogenesis (Blais et al., 2005; Cao et al., 2006). At an early differentiation stage, MyoD alone activates direct downstream genes and then maintains activation

of the myogenic program (Blais et al., 2005; Cao et al., 2006). However, how MyoD acts to repress transcriptional programs, such as those mediated by Id proteins, which would otherwise inhibit skeletal myogenesis, is not well known.

One postgenomic strategy used to identify molecular networks functioning in tissue development is microarray analysis of individual cell types or tissues followed by in situ hybridization to identify temporal and spatial gene expression patterns. A disadvantage of this approach is that it does not detect gene expression restricted to small areas. In addition, it is difficult to identify common or specific developmental molecular networks from in situ hybridization data collected separately by independent researchers.

To obtain comprehensive spatiotemporal profiles of transcription factors during embryonic development, we created a whole-mount in situ hybridization database, called "EMBRYS" (http://embrys.jp/), for 1520 transcription factors and cofactors, using whole mouse embryos at midgestational stages (Embryonic Days [E] 9.5, 10.5, and 11.5), during which striking dynamic changes in pattern formation and organogenesis occur. Using this database, we annotated gene expression patterns underlying critical developmental events. Specifically, we identified a gene cluster expressed during limb skeletal myogenesis. Among 43 transcription regulators showing myogenic expression in the limb bud, we identified the transcriptional repressor RP58 and found that myogenesis was severely perturbed in *RP58* null mice, in C2C12 cells expressing *RP58* shRNA, and in *RP58* null fibroblasts, in which myogenesis is induced by ectopic expression of MyoD. We utilized high-throughput, cell-based transfection assays and found that MyoD promotes *RP58* gene expression. DNA microarray analysis with bioinformatics identified *Id2* and *Id3* as direct RP58 targets. Overall our combined systems approach identified RP58 as an effector included in MyoD-activated positive feedback and enabling progression of skeletal myogenesis by repressing expression of *Id2* and *Id3*, inhibitors of myogenesis.

RESULTS

Database Construction

To identify and characterize effectors of the transcriptional network regulating developmental processes, we developed a web-based comprehensive WISH database for transcriptional regulators using E9.5, 10.5, and 11.5 mouse embryos (Figure 1). To do so, we combined published databases (Kanamori et al., 2004; Thomas et al., 2003) to generate a list of 2911 transcription regulators (see Figure S1 available online). We then prepared from cDNA libraries 1520 digoxigenin-labeled RNA probes (Table S1). Using WISH results, we constructed a database, termed "EMBRYS", covering these 3 embryonic days (Figure 1A and Tables S1–S3, available at http://embrys.jp/embrys/html/MainMenu.html).

Annotation of Gene Expression

We annotated expression patterns of each gene in the EMBRYS database as defined in Figures 1B–1D and Table S4. In particular, WISH enables analysis of limb development in three-dimensional axes during embryogenesis and provides highly precise gene expression information (Kawakami et al., 2003; Mariani and Martin, 2003). Our analysis indicated that 962 genes showed detectable signals in the entire embryo over these 3 days and that 691 were expressed in the limb bud. Information relative to these expression patterns is summarized in Table S5.

RP58 Is Expressed in Skeletal Muscle Tissues and in C2C12 Cells

Based on EMBRYS, we identified 43 genes showing myogenesis-related expression patterns in the limb bud from E9.5–E11.5 (Table 1 and Figure S2). Among them, *RP58* was one of the few genes whose function in skeletal myogenesis has not been previously characterized (Figure 2A).

RP58 mRNA expression was first detectable at E11.5 in the limb bud in a pattern typical of myogenesis (Figure 2A) and coincident with upregulation of *Myog* (Figure 2A). By contrast, *Pax3*, a marker of myogenic precursors (Bober et al., 1994; Williams and Ordahl, 1994), is expressed in the limb bud at E9.5, and *Myf5* and *MyoD* are expressed at E10.5 (Figure 2A). In *Splotch* mutant mice ($Pax3^{Sp/Sp}$), in which muscle tissues do not form in limb buds because of defects in migration of myogenic precursors from somites (Daston et al., 1996), no *RP58* signals were observed in limb buds by WISH analysis, confirming myogenic expression of *RP58* (Figure S3). *RP58* was also expressed in brain and spinal cord, as previously reported (Ohtaka-Maruyama et al., 2007; Okado et al., 2009). Collectively, these data indicate that RP58 is a potential downstream target of muscle lineage and determination factors.

We used C2C12 muscle cells (Blau et al., 1983; Yaffe and Saxel, 1977) to monitor RP58 expression during muscle differentiation in vitro. RP58 mRNA and protein expression was upregulated at early stages of C2C12 differentiation (on differentiation day 0 [0d]; Figures 2B and 2C), with an expression pattern overlapping that of *Myog* and prior to expression of late muscle markers, such as *Ckm* (creatine kinase, muscle). These data suggest that *RP58* is an early muscle differentiation gene.

RP58 Knockdown Results in Differentiation Defects in Skeletal Muscle

We first examined the role of RP58 in myogenesis by generating C2C12 cell lines stably expressing *RP58* shRNA. RP58 knockdown in C2C12 myoblasts (on differentiation day 4 [4d]; Figure 3A) severely impaired their ability to form multinucleated myotubes and to induce the late-muscle gene Myosin Heavy Chain (MyHC) at differentiation day 4 (4d) (Figures 3B and 3C).

To determine the role of RP58 during skeletal myogenesis in vivo, we analyzed skeletal muscle phenotypes in *RP58* null mice (Okado et al., 2009). *RP58* null mice died immediately after birth. At E18.5 the size of wild-type and null embryos was equivalent (data not shown); however, muscle differentiation of *RP58* null mice was severely disrupted, as revealed by hematoxylin and eosin (H&E) staining (Figure 3D and 3E and Figure S4). In knockout mice, regions of the hindlimb normally populated by multinucleate muscle fibers instead exhibited large areas of mononucleate cells and showed a striking reduction in the number of myofibers (Figure 3D and Figure S4). A dramatic reduction in the size of the diaphragm and other skeletal muscle was apparent in $RP58^{-/-}$ mice, as compared with wild-type mice (Figure 3E and Figure S4). MyHC and troponin T-positive cells in $RP58^{-/-}$ mice are significantly reduced, although the few

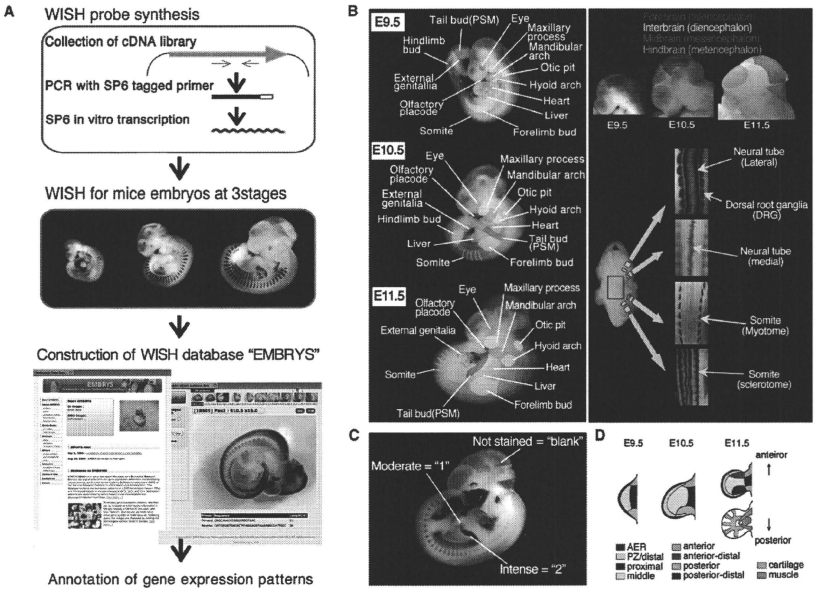

Figure 1. Myogenic Expression of RP58 Based on the WISH Database

(A) Flow chart of database construction.

(B) Representation of annotated gene expression. Gene expression detected by WISH was evaluated in several anatomical structures. (Left) Lateral views of embryos at E9.5, 10.5, and 11.5. Hybridization signals detected in colored areas were evaluated visually. Magnification of each photo is not uniform. (Upper Right) Anatomical drawing of the brain at each stage. (Bottom Right) Dorsal view of trunk. Boxed area is enlarged and detailed structures are visualized by WISH performed with markers of each structure. PSM, presomitic mesoderm.

(C) Signal intensity is evaluated as follows: 2, intense (as in the posterior part of the forelimb bud); 1, moderate (as in Progress Zone, PZ); or blank, no signal or not determined. Areas showing no detectable signal, such as the regions of brain, are annotated "Not Stained," and staining that could not be interpreted is evaluated as "Not Determined" and indicated as blank cells in Table S4.

(D) Gene expression patterns in the developing limb bud are shown in detail, and colored areas are individually evaluated. AER, apical ectodermal ridge; PZ, progress zone.

remaining myofibers in the limb field showed normal morphology (Figure S4).

Next, to determine whether muscle impairment seen in *RP58* null mice was caused by inhibition of myogenic precursor migration from the dermomyotome to appendicular muscle tissues, we examined expression of *Pax3*, a marker of the migratory myogenic precursors, in *RP58* null mice. The *Pax3* expression pattern was not altered in limb of *RP58* knockout mice at E10.5, indicating that migration of muscle precursors to the limb field was not affected by loss of *RP58* (Figure S5).

Cell-Based HTS Reveals that MyoD Functions Upstream of RP58

Next we asked what upstream factors promote RP58 expression in muscle cells. To do so, we generated a system in which 6049 cDNA expression vectors were arrayed on 384-well plates and used to transfect 293T cells along with a reporter plasmid containing RP58 control sequences, and monitored for luciferase activity. To construct the reporter, the human *RP58* promoter sequence (−5K to +3K) was compared with that of mouse, chimpanzee, dog, chicken, *Xenopus*, and zebrafish by VISTA browser (Frazer et al., 2004). A 3.4Kb region (from −3180 to +170 of mouse *RP58*), which is highly conserved in mammalian species, was identified and subcloned into the pGL4.12 luciferase vector in front of a luciferase cassette (Figure 4A).

On the first screen, 11 of 6049 clones showed a greater than 1.5-fold increase in *RP58* promoter activity compared with empty plasmid controls. An additional screen was performed using both the RP58 3.4K and a shorter 1.6K promoter (−1596 to −1). This screen identified the bHLH proteins MyoD,

Table 1. Profile of Genes Expressed in Limb Muscle

	NCBI Gene ID	Symbol	Alternative	Domain	Expression
1	218490	**Btf3**	1700054E11Rik		2
2	59035	**Carm1**	Prmt4		1
3	107951	**Cdk9**	PITALRE		1
4	56449	**Csda**	MSY4		2
5	269713	**Clip2**	Cyln2		1
6	13194	**Ddb1**	AA408517		1
7	226049	**Dmrt2**	Terra	DM	1
8	15205	**Hes1**	Hry	bHLH	1
9	55927	**Hes6**	AI326893	bHLH	2
10	15384	**Hnrnpab**	Hnrpab		2
11	15516	**Hsp90ab1**	Hspcb		2
12	15902	**Id2**	Idb2	bHLH	2
13	15903	**Id3**	Idb3	bHLH	2
14	16468	**Jarid2**	Jmj	ARID	2
15	50868	**Keap1**	INRF2		1
16	16814	**Lbx1**	Lbx1h	Homeobox	2
17	17220	**Mcm7**	Mcmd7		2
18	17258	**Mef2a**	A430079H05Rik	MADS-box	1
19	17260	**Mef2c**	5430401D19Rik	MADS-box	2
20	17261	**Mef2d**	MGC31718	MADS-box	1
21	17283	**Men1**	AW045611		1
22	17286	**Meox2**	Mox2	Homeobox	2
23	18432	**Mybbp1a**	p67MBP		2
24	17869	**Myc**	c-myc	bHLH	2
25	17877	**Myf5**	Myf-5	bHLH	2
26	17927	**Myod1**	MyoD	bHLH	2
27	17928	**Myog**	Myogenin	bHLH	2
28	110109	**Nop2**	Nol1		2
29	23967	**Osr1**	Odd1	ZF C2H2	2
30	18505	**Pax3**	splotch	Homeobox	2
31	18742	**Pitx3**	Ptx3	Homeobox	2
32	19401	**Rara**	Nr1b1	NR	2
33	56190	**Rbm38**	Rnpc1		1
34	67097	**Rps10**	2210402A09Rik		1
35	20471	**Six1**	BB138287	Homeobox	2
36	12180	**Smyd1**	Bop	ZF MYND	2
37	64406	**Sp5**		ZF C2H2	2
38	20901	**Strap**	AW557906		1
39	21413	**Tcf4**	E2-2	bHLH	2
40	21416	**Tcf7l2**	Tcf-4	HMG	2
41	21681	**Thoc4**	REF1		2
42	22608	**Ybx1**	YB-1		2
43	30928	**Zfp238**	RP58	ZF C2H2	2

Total profiles of genes expressed in the E11.5 muscle-forming region. Forty-three genes were identified as muscle transcription factors by EMBRYS database. NCBI gene ID (http://www.ncbi.nlm.nih.gov/), gene symbol, alternative gene name, representative predicted DNA binding domain (domain), and intensity of expression in limb muscle (expression) based on EMBRYS analysis are shown in each column, respectively. Although migration of myogenic cells from trunk to forelimb starts around E9.5, we cannot identify the signal as being derived from muscle cells at E9.5 and E10.5 limb middle mesenchyme. However, we did classify muscle expression genes based on expression patterns of *MyoD* and *Myog* at E11.5 (cf Figure 2A; Figure S2; Table S4). We screened, collected, and annotated "muscle genes" using this pattern in E11.5 limb bud. Thus, these 43 genes are identified. In the Expression column, "2" indicates an intense signal and "1" indicates moderate expression in limb muscle (cf Figure 1C). Abbreviations: DM, dsx and mab-3; bHLH, basic helix-loop-helix; ARID, AT-rich interaction domain; MADS, MCM1, Agamous, Deficiens, and SRF; ZF, zinc finger; NR, nuclear receptors; HMG, high-mobility group. Blank indicates genes do not encode TFs.

NEUROG1, NEUROG2, and NEUROD1 as transcriptional activators of the *RP58* promoter (Figure 4B). All of these proteins increased the 3.4K promoter activity more than 5-fold and the 1.6K promoter activity more than 20-fold (Figure 4B). These data place RP58 as a potential target of muscle- and neural-specific bHLH factors and suggest that RP58 functions in transcriptional networks regulating both skeletal myogenesis and neurogenesis. Sequence-specific bHLH transcription factors, such as MyoD, typically activate transcription by binding to E-box sequences (CANNTG). A TFSEARCH (http://mbs.cbrc.jp/research/db/TFSEARCH.html) identified three E-boxes (E1-3) within the 1.6K *RP58* promoter region (Figure 4C). Disruption of E1 or E2, but not E3, by point mutations reduced MyoD-dependent promoter activity, and disruption of both E1 and E2 almost completely abrogated MyoD-dependent promoter activity (Figure 4C), indicating that E1 and E2 are critical for MyoD-dependent *RP58* expression. To investigate MyoD binding to the E1 and E2 sites, we undertook ChIP analysis using an anti-MyoD antibody in C2C12 cells cultured in growth medium (GM) or differentiation medium (DM) (Figure 4D). We found that MyoD bound to the RP58 promoter in DM more strongly than in GM and that the histone acetylation state of *RP58* in DM was higher than in GM.

Significantly, MyoD and its target, Myog, are both expressed in the myotome of *RP58* null mice at the protein level at E10.5 (Figure 4E). Furthermore, *RP58* mRNA is detected in *Myog* KO mice (Figure S6). These results suggest that MyoD-Myog pathway and MyoD-RP58 pathway may represent two distinct branches functioning in skeletal myogenesis.

Id2 and Id3 Are Directly Repressed by RP58 in Myogenesis

RP58 was originally identified as a DNA-binding transcriptional repressor associated with transcriptionally silent heterochromatin (Aoki et al., 1998). However, its physiological target genes were unidentified. We confirmed that RP58 functions as a transcriptional repressor in C2C12 cells using a putative RP58 binding sequence reporter system (Fuks et al., 2001) (data not shown). To identify RP58-regulated genes involved in myogenesis, profiling experiments were performed comparing RNA derived from C2C12 cells with or without expression of *RP58* shRNA. In C2C12 cells stably expressing shRNA-*RP58*, 271 genes were upregulated relative to control cells (Figure 5A and Table S6). Given its repressor function, these upregulated genes are potential targets of RP58 repression. In parallel, we

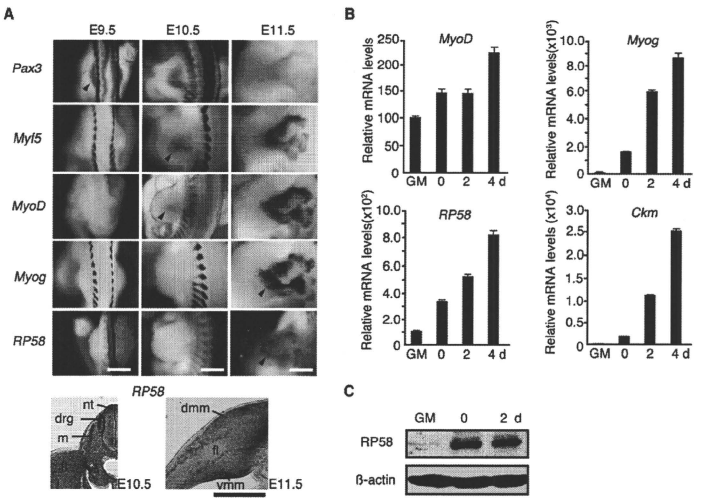

Figure 2. RP58 Expression in Mouse Limb Bud and in C2C12 Culture

(A) Expression patterns of muscle-related transcription factors (*Pax3*, *Myf5*, *MyoD*, and *Myog*) and *RP58* in mouse limb bud at E9.5, 10.5, and 11.5, as determined by WISH. At the bottom are sections of an E10.5 (Left) or E11.5 (Right) embryo showing *RP58* expression. Abbreviations: m, myotome; drg, dorsal root ganglia; nt, neural tube; dmm, dorsal muscle mass; vmm, ventral muscle mass; fl, forelimb. Bar, 500 μm.

(B) Real-time PCR analysis of *RP58* and myogenesis-associated genes in C2C12 cells cultured in GM or DM for 0, 2, or 4 days (d). Error bars, SEM (n = 3).

(C) Western blotting for RP58 during C2C12 cell myogenic stages.

evaluated dynamic gene expression patterns during myogenesis by microarray at four different differentiation stages of wild-type C2C12 cells (GM, and differentiation days 0, 2, and 4). This analysis identified 399 genes downregulated as differentiation proceeded (Figure 5A and Table S7). Strikingly, we observed high overlap between those genes and genes upregulated in C2C12 cells expressing *RP58* shRNA (195 genes; Figure 5A; Tables S8, S10, and S11). To identify direct targets of RP58 among the above candidates, we screened for predicted RP58 binding sites in candidate promoters (from −7K to +3K; Table S9). If RP58 binds to such sequences, the binding sites would likely be conserved. To search for such sites, sequences were compared among mouse, human, and opossum using UCSC BLAT (Kent, 2002). Highly conserved consensus RP58 binding sequences were seen in four genes (*Id2*, *Id3*, *Pea3* [*Etv4*], and *Tubb3*; Figure 5A), all of which were significantly downregulated in differentiating C2C12 cells and upregulated in *RP58* knockdown C2C12 cells (Figure 5B; data not shown).

Among them, *Id2* and *Id3* were of particular interest as they are known inhibitors of skeletal myogenesis (Chen et al., 1997; Kurabayashi et al., 1994; Melnikova and Christy, 1996). We confirmed that constitutive overexpression of *Id2* and *Id3* in C2C12 cells severely inhibits fusion of myoblasts into myotubes, in agreement with other reports (Figure S7; Chen et al., 1997; Kurabayashi et al., 1994; Melnikova and Christy, 1996). Significantly, infection of C2C12 cells with RP58-expressing adenovirus reduced *Id2* and *Id3* expression levels compared with control adenovirus (Figure 5C).

Our EMBRYS database also detected *Id2* and *Id3* mRNA expression in limb skeletal muscle (Table 1 and Figure S2). *RP58* is further expressed in limb muscle at E12.5 and 13.5, but *Id2* and *Id3* expression is downregulated at these stages (Figure S8). Consistently, we detected abnormally higher levels of *Id2* and *Id3* in E18.5 diaphragm muscle from *RP58* null mice (Figure 5D). On the contrary, decreased levels of *Ckm* mRNA in the same samples further support a functional link between RP58-mediated repression of Id proteins and activation of late stages of skeletal myogenesis (Figure 5D). The upregulated *Id2* and *Id3* expression was also observed at earlier stages of myogenesis in the somite at E10.5 and limb at E13.5 of *RP58* null mice compared with wild-type mice (Figure 5E).

To determine whether Id2 and Id3 are directly downregulated by RP58, we performed transfection assays with luciferase reporters and ChIP assays (Figures 6A–6C). The activities of a luciferase reporter gene fused to putative RP58 binding sites (in *Id2* −2576 to −2966 or in *Id3* −3318 to −3028) were reduced

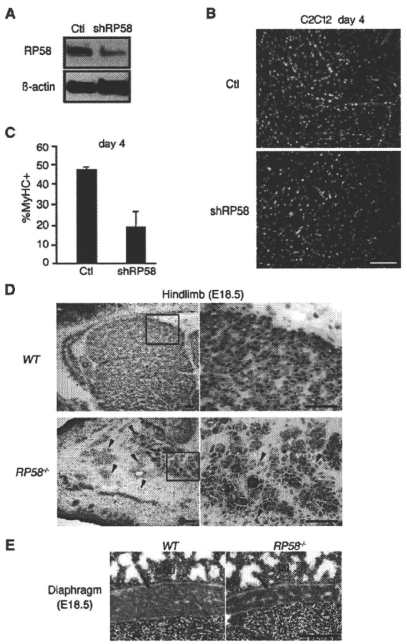

Figure 3. RP58 Knockdown Inhibits Myogenesis

(A) Western blotting for RP58 in C2C12 lines stably expressing *RP58* shRNA (shRP58) or control shRNA (Ctl) on differentiation day 2.

(B) Immunocytochemistry for MyHC and DAPI staining in C2C12 lines stably expressing *RP58* shRNA (shRP58) or control shRNA (Ctl) on differentiation day 4. Bar, 200 μm.

(C) Percentage of MyHC-positive nuclei in RP58 knockdown (shRP58) or control (Ctl) C2C12 cells of (B) in three independent fields. Error bars, SD ($n = 3$).

(D) H&E staining of hindlimb muscles from *WT* and *RP58*$^{-/-}$ mice (E18.5). Higher magnifications of boxed regions in left panels are shown in right panels. Arrowheads indicate an abnormal population of mononucleate cells in *RP58*$^{-/-}$ skeletal muscle tissues. Bar, 50 μm.

(E) Haematoxylin and eosin staining of diaphragm from *WT* and *RP58*$^{-/-}$ mice (E18.5, arrow). Lu, lung; Li, liver. Bars, 50 μm.

following RP58 expression in C2C12 cells (Figures 6A and 6B). ChIP analysis of C2C12 cells using an anti-Flag antibody showed that Flag-RP58 bound to chromatin of *Id2* and *Id3* regulatory sequences (Figure 6C). We further explored the "MyoD-RP58-Id2, 3" cascade by evaluating the ability of MyoD to activate the myogenic program in 10T1/2 fibroblasts derived from either wild-type (WT) or *RP58*$^{-/-}$ mouse embryonic fibroblasts (MEF). Ectopic expression of MyoD efficiently converts WT 10T1/2 fibroblasts into muscle cells, as previously reported (Weintraub et al., 1989), but fails to activate the myogenic program in *RP58*$^{-/-}$ 10T1/2 fibroblasts (Figure 6D). The resistance of *RP58*$^{-/-}$ 10T1/2 fibroblasts to MyoD-mediated myogenic conversion correlated with increased levels of *Id2* and *Id3*, which are otherwise downregulated by ectopic expression of MyoD in WT 10T1/2 fibroblasts (Figure 6D). Knockdown of Id2 and Id3 by siRNA restored MyoD-dependent activation of the myogenic program in *RP58*$^{-/-}$ 10T1/2 fibroblasts (Figure 6E) leading to the formation of multinucleated myotubes (Figure S9).

These data support the existence of MyoD-activated positive feedback that allows the progression of skeletal myogenesis, via RP58-mediated transcriptional repression of two key inhibitors of muscle differentiation, *Id2* and *Id3* (Figure 6F).

DISCUSSION

Our systems approach, in which WISH database construction and annotation were integrated with cell-based, high-throughput transfection screening and microarray analysis, identified RP58 as part of a MyoD-activated positive feedback mechanism that enables progression of skeletal myogenesis by repressing myogenic inhibitors. EMBRYS construction successfully provided annotated gene expression information that led to identification of RP58 as a critical transcription factor in the myogenic program. In addition, application of cell-based high-throughput transfection screening to identify factors that upregulate specific promoters constituted an unbiased functional assay. Overall we have determined a pathway whereby the repressor RP58 negatively regulates Id expression.

Advantages of the WISH Database, EMBRYS

Compared with microarray analysis, the systematic in situ hybridization database presented here provides more detailed information on the spatial regulation of gene expression and allows identification of discrete clusters of transcribed genes. This advantage was demonstrated by previous studies of brain tissues (Gray et al., 2004; Lein et al., 2007). The importance of identifying gene clusters in each tissue's dynamic development was also emphasized by the recent discovery of reprogramming techniques to generate iPS cells (Takahashi and Yamanaka, 2006) and β-cells (Zhou et al., 2008), in which combined forced expression of transcription factors appearing in each differentiation program can alter cell fate and differentiation status.

Our EMBRYS database combined with WISH images of E9.5, E10.5, and E11.5 mouse embryos, which annotates gene expression patterns, is advantageous in identifying embryonic transcriptional networks compared to existing techniques (Figure 1, Tables S1–S5). Using this approach, we identified 43 genes showing myogenic expression patterns (Table 1 and Figure S2). We also annotated dynamic gene expression patterns in other tissues and organs, which should be useful to analyze other developmental or regenerative networks (Figure 1B and Tables S4 and S5).

Limb development in particular is an excellent model to study patterning and examine molecular networks underlying three dimensional axes because of the existence of well characterized signaling centers such as the apical ectodermal ridge (AER), an ectodermal structure at the most distal end of the limb

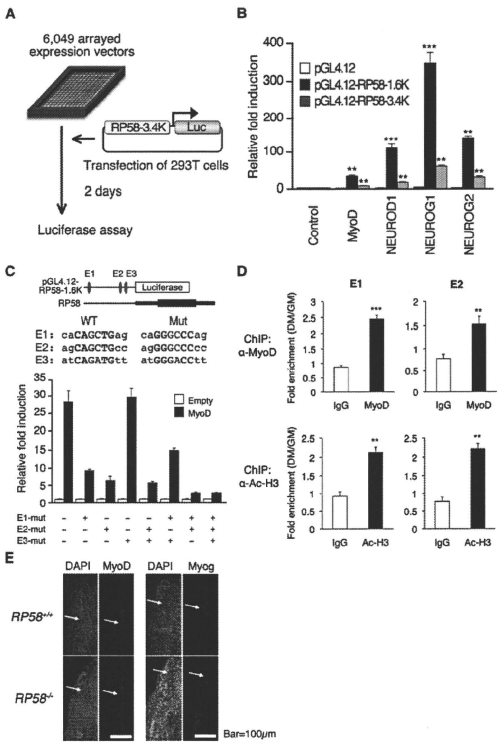

Figure 4. High-Throughput Transfection Screening of RP58 Initiators

(A) HTS scheme.

(B) Luciferase activity of pGL4.12, pGL4.12-RP58-1.6K, or pGL4.12-RP58-3.4K reporters in 293T cells transfected with MyoD-, NEUROD1-, NEUROG1-, NEUROG2-expressing vectors or empty vector. Error bars, SD (n = 3).

(C) (Upper panel) Reporter vector pGL4.12-RP58-1.6K and the corresponding upstream region of *RP58*. Relative positions and sequences of E-boxes E1, E2, and E3, which are potential MyoD binding sites, are shown with mutations introduced into these regions. (Lower panel) Luciferase activity of various reporters, mutated either individually or in combination, in 293T cells transfected with MyoD-expressing or empty vector. Error bars, SD (n = 3).

(D) Quantitative ChIP analysis using anti-MyoD or anti-acetyl-histone 3 antibody (α-Ac-H3) on E1 and E2, potential MyoD binding sites on *RP58* promoter, in C2C12 cells cultured in GM or DM. Error bars, SEM (n = 3).

(E) Immunohistochemistry of transverse sections of forelimb level somites in E10.5 wild-type (WT) or *RP58*$^{-/-}$ mice using anti-MyoD or -Myog antibodies. Counterstaining was performed using DAPI. Bar, 100 μm.

however, these methods are limited to identifying direct targets. Application of a comprehensive set of cDNAs in an expression library allows high-throughput screening not only for direct transcriptional regulators but also for other factors, such as cell-signaling molecules, receptors, or growth factors (Iourgenko et al., 2003).

Here we utilized around 6000 arrayed and addressable cDNA clones, which allowed systematic, efficient, and unbiased screening of cDNAs' encoding factors that could activate the *RP58* promoter (Figure 4A). Our screen revealed MyoD, NEUROG1, NEUROG2, and NEUROD1 as potential activators of the *RP58* promoter. Consistent with our findings, recently two independent genome-wide approaches identified RP58 as a downstream target of MyoD (Di Padova et al., 2007) and Neurod1 and Neurog2 (Seo et al., 2007). Thus, we and others have confirmed that RP58 expression in myogenesis and neurogenesis is likely regulated by tissue-specific bHLH transcription factors. Our findings also support the idea that genome-wide functional approaches are useful to identify critical molecular networks functioning in different tissues or developmental stages.

Di Padova et al. have also indicated that acetylation-activated MyoD promotes RP58 expression in the early phase of myogenesis (Di Padova et al., 2007), when we found MyoD to be recruited to the RP58 promoter (Figure 4D). Chromatin association of MyoD and activation of downstream genes is typically promoted by recruitment of p300 and PCAF acetyltransferases (McKinsey et al., 2001; Puri et al., 1997; Sartorelli et al., 1999) and other chromatin-modifying complexes (Guasconi and Puri, 2009). In myoblasts, most of the promoters are not occupied by MyoD, possibly because of the high levels of Ids which

indispensable for induction of proximodistal limb outgrowth (Saunders, 1948), and the zone of polarizing activity (ZPA), a posterior margin of the limb important for determining anteroposterior patterning (Riddle et al., 1993; Wolpert, 1969). We extensively analyzed gene expression patterns in limb fields relative to these axes (Figure 1D). Thus the EMBRYS database provides us a means to examine molecular networks functioning in both differentiation and polarity programs (Table S4).

Cell-Based High-Throughput Functional Screening Identifies MyoD as an RP58 Activator

Currently, signals activating gene expression are identified by examining potential transcription factor binding sequences in a specific promoter using bioinformatics and cell-based reporter assays. If a factor's potential recognition motif is unknown, one-hybrid or south-western screening can be used to identify molecules directly associated with the specific sequence;

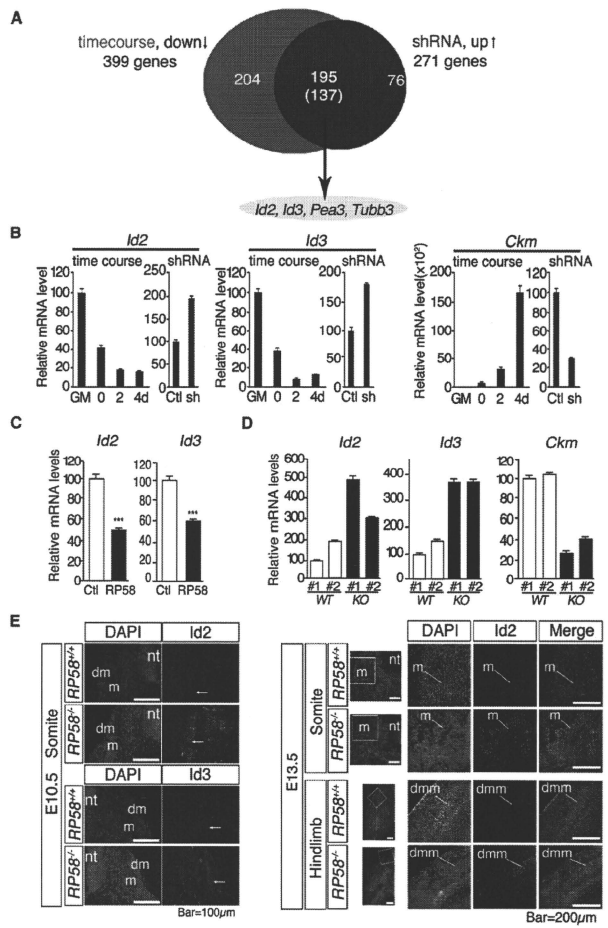

Figure 5. Microarray Analysis for RP58 shRNA-Expressing C2C12 Cells

(A) Venn diagram of genes upregulated by treatment with RP58 shRNA ("shRNA") and downregulated as C2C12 cells differentiate ("timecourse").

(B) Real-time PCR of *Id2*, *Id3*, and *Ckm* in C2C12 cells cultured in growth (GM) or differentiation (DM) medium at 0, 2, or 4 days (d) or in control- (Ctl) or RP58- (sh) shRNA-expressing C2C12 cells. Error bars, SEM (n = 3).

(C) Real-time PCR of *Id2* and *Id3* in C2C12 cells infected with RP58-expressing or control adenovirus. Error bars, SEM (n = 3).

(D) Real-time PCR of *Id2*, *Id3*, and *Ckm* in diaphragm of *RP58* KO or *WT* mice (E18.5). Error bars, SEM (n = 3).

(E) Immunohistochemistry of transverse section of wild-type ($RP58^{+/+}$) and RP58 KO ($RP58^{-/-}$) mice at E10.5 (Left panel) and E13.5 (Right panel), using anti-Id2 (for both E10.5 and E13.5) or -Id3 (for E10.5) antibodies. Counterstaining was performed using DAPI. In E13.5, boxed areas are enlarged in the right panel. Bars, 100 μm (E10.5), and 200 μm (E13.5), respectively.

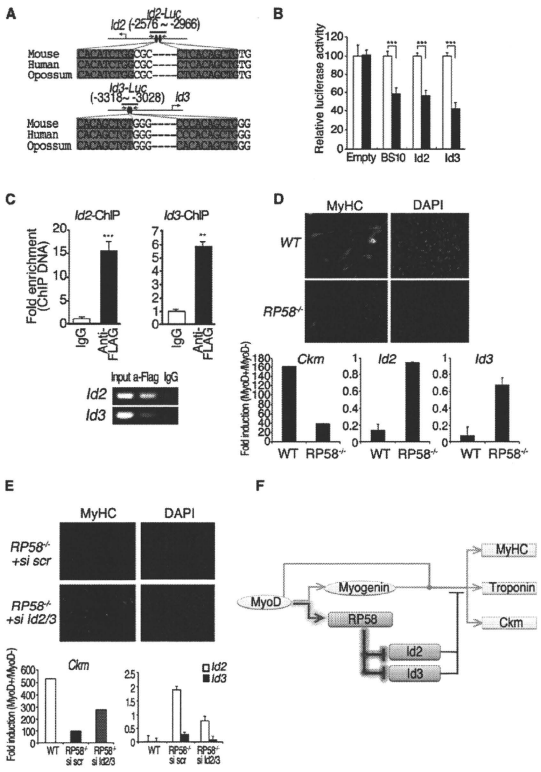

Figure 6. Id2 and Id3 Are Direct Targets of RP58

(A) Location and sequence (in mouse, human, and opossum) of highly conserved putative RP58 binding sites in Id2 (upper) or Id3 (bottom) promoters.

(B) Luciferase activity of TK-Luc (Empty), BS10-Luc (BS10), Id2-Luc (Id2), or Id3-Luc (Id3) reporters in C2C12 cells transfected with RP58-expressing or empty vector. Error bars, SD (n = 3).

(C) Quantitative ChIP assay in C2C12 cells infected with Flag-RP58-expressing adenovirus. Error bars, SEM (n = 3).

(D) (Upper) Immunofluorescence for MyHC expression in WT or RP58 null 10T1/2 fibroblasts in which the myogenic program is activated upon ectopic expression of MyoD on differentiation day 3 (3d). (Lower) Real-time PCR of *Ckm*, *Id2*, and *Id3* in WT or RP58 null 10T1/2 fibroblasts expressing MyoD on differentiation day 3 (3d). Error bars, SEM (n = 3).

(E) (Upper) Immunofluorescence for MyHC expression in WT or RP58 null 10T1/2 fibroblasts in which the myogenic program is activated upon ectopic expression of MyoD and siRNA-mediated downregulation of Id2 and Id3 on differentiation day 2 (2d). (Lower) Real-time PCR of *Ckm* (Left) and *Id2*, *Id3* (Right) in WT or RP58 null 10T1/2 fibroblasts in the same conditions described above on differentiation day 2 (2d). Error bars, SEM (n = 3).

(F) Proposed myogenesis regulatory network.

2006; Di Padova et al., 2007). For instance, Myog is expressed at an early stage of differentiation, while Ckm and MyHC are considered late muscle genes. Recent work indicates that the ability of MyoD to support transcription of late genes is tightly controlled by downstream early target genes (Blais et al., 2005; Cao et al., 2006). On the other hand, earlier work established that the ability of MyoD to activate late stage genes is antagonized by Id proteins. Overexpression of *Id2* and *Id3* in muscle cells inhibits myoblast fusion to myotubes (Figure S7) and represses expression of late myogenic targets, such as Ckm and MyHC (Benezra et al., 1990; Jen et al., 1992; Langlands et al., 1997; Melnikova et al., 1999; Neuhold and Wold, 1993). Our finding of an Ids-repressing pathway by MyoD-dependent RP58 signaling may play a critical role for temporally patterned expression of early and late genes.

preclude MyoD heterodimerization with E12/47, an event required for robust MyoD binding to DNA (Guasconi and Puri, 2009). Taken together, these data suggest that MyoD activates RP58 in DM more strongly than in GM because it uses a mode of activation similar to that of other "differentiation genes," such as Myogenin.

RP58, a Transcriptional Repressor of Id2 and Id3 in the Myogenic Program

We found that *RP58* directly represses the *Id2* and *Id3* expression. Extensive evidence indicates that temporal control of muscle gene transcription by direct activation of downstream targets (early genes) by MyoD enables subsequent transcription of late genes (Cao et al., 2006; Penn et al., 2004). MyoD directly upregulates numerous targets, including Myog, Ckm, and MyHC, with distinct kinetics (Blais et al., 2005; Cao et al.,

It has been reported that the Ids reduction during myogenesis is initiated by serum depletion in vitro (Chen et al., 1997; Kurabayashi et al., 1994; Wu and Lim, 2005). We detected reduced levels of Id2 and Id3 in *RP58* knockdown C2C12 cells (data not shown), indicating the importance of RP58-mediated downregulation of *Id2* and *Id3*, as mechanism of maintenance of Ids repression that is initiated by serum depletion. This is consistent with the in vivo data showing that in *RP58* null embryos *Id2* and *Id3* expression is upregulated in muscle regions (Figure 5E). Here

we propose that this Ids downregulation is governed by two independent pathways: (1) In proliferating myoblasts (cultured in high serum-containing medium), *Id2* and *Id3* expression is induced by serum mitogens, possibly via different mechanisms (Chen et al., 1997; Kurabayashi et al., 1994; Wu and Lim, 2005); (2) MyoD-dependent RP58 signaling maintains *Id2* and *Id3* in a repressed state.

Taken together, identification of RP58 as a critical effector in a myogenic feedback mechanism is intriguing because it suggests that MyoD activates parallel programs, leading to both "activation" and "repression" of distinct subsets of genes and permitting progression of skeletal myogenesis toward late differentiation stages (Blais et al., 2005; Cao et al., 2006; Chen et al., 1997).

EXPERIMENTAL PROCEDURES

EMBRYS Construction

The list of transcription factors and cofactors was created as described in Figure S1. Whole-mount in situ hybridization was performed as described (Yokoyama et al., 2008). DIG-RNA signals were photographed under a light microscope (OLYMPUS SZX12) equipped with a CCD camera (OLYMPUS DP70). Specimens were embedded in agarose gel to capture images from any direction. Generally, three photos were taken for each embryo: the embryo at low magnification, the forelimb and hindlimb at medium magnification, and the forelimb at high magnification. Additional photos were taken if gene expression was clearly detected in specific tissues (i.e., brain, spinal cord, pharyngeal arches, eye, olfactory placode, somite, heart, liver, tail bud, otic pit, external genitalia) at appropriate magnifications. Images were converted to .jpeg format and deposited in the gene expression pattern database "EMBRYS" (http://embrys.jp/).

Constructs

pGL4.12-RP58-3.4K or pGL4.12-RP58-1.6K were constructed by inserting the −3180 to +170 or −1596 to −1 region of mouse *RP58* into the pGL4.12 vector (Promega). Mutations were introduced into various sites between −1255 and −1250 (E1), −220 and −215 (E2), and −190 and −185 (E3) of pGL4.12-RP58-1.6K using a QuikChange site direct mutagenesis kit (Stratagene). pGL-TK was constructed by inserting the TK promoter of pRL-TK (Promega) into the BglII-HindIII site of pGL4.12. BS10-Luc, a reporter containing 10 copies of RP58 binding sites fused to the TK promoter and the luciferase gene, was constructed by ligating the KpnI-SacI fragment of BS10-pGL2C (Aoki et al., 1998) into the KpnI-SacI site of pGL-TK. Id2-Luc or Id3-Luc vectors were constructed by inserting the −2576 to −2966 region of *Id2* or the −3318 to 3028 region of *Id3*, respectively, into pGL-TK. Expression vectors were constructed by inserting respective ORFs into pcDNA3.1 (+) (Invitrogen), p3xFlag-CMV-7.1 (SIGMA) or pcDNA3-HA, in which an HA-tag was inserted upstream of the multicloning site. A vector expressing *RP58* shRNA was constructed using the BLOCK-iT Inducible H1 RNAi Entry Vector Kit (Invitrogen). Three RP58 target sequences were designed using Invitrogen webpage guidelines. They were: 5′-GCTTCATGCAGCATGTATTTC-3′, 5′-GCCCAGTGA TGAAGATGAAGG-3′, and 5′-GCTAGCAGCTGCCAGTTATCT-3′. Flag-RP58-expressing adenovirus vector was produced by ViraPower Adenoviral Expression System (Invitrogen).

Cell Culture, Transfection, and Adenovirus Infection

C2C12 murine skeletal muscle cells and 293T human embryonic kidney cells were purchased from American Type Culture Collection (ATCC). Cells were maintained in Growth Medium (GM: DMEM supplemented with 10% FBS). For C2C12 culture, cells were grown in GM and, after reaching full confluence, medium was switched to Differentiation Medium (DM: DMEM supplemented with 2% horse serum) and further incubated. All C2C12 cell culture was performed using cells within five passages. Transfection was performed using Lipofectamine 2000 (Invitrogen). Stable transfectants were obtained by selection of cells using G418 or Zeocine for 2 weeks. Adenovirus infection was performed in C2C12 cells at a multiplicity of infection (MOI) of 50–100, and cells were incubated 2 days in DM after reaching confluence and then assayed by real-time PCR or ChIP.

RNA Isolation and Quantitative Real-Time PCR

Total RNAs were isolated from cultured cells or tissue using ISOGEN (Nippongene) and reverse transcribed using Ready-To-Go You-Prime First-Strand Beads (GE Healthcare). cDNAs were used for quantitative real-time PCR, which was performed using the SYBR GREEN PCR Master Mix (Applied Biosystems). *Gapdh* expression served as a control for mRNA expression. Gene expression changes were quantified using the delta-delta C_T method. Primer sequences are available upon request.

Histology, Immunostaining, and Western Blotting

Hindlimbs from E18.5 were dissected, embedded in tragacanth gum (Wako), and snap-frozen in liquid nitrogen-cooled isopentane, followed by cryostat sectioning at 6 μm. Whole E13.5 embryos were embedded in OCT compound (Sakura Finetek) and frozen rapidly in liquid nitrogen. Specimens were sectioned at 10 μm. Cryosections were air-dried and stained with H&E. For E10.5 myotome immunohistochemistry, embryos were fixed by 4% paraformaldehyde (PFA) in PBS and embedded in paraffin, followed by microtome sectioning at 7 μm. Anti-MyoD (1:100; clone 5.8A, BD), anti-Myog (1:50; F5D, DSHB), anti-Id2 (1:100; C-20, sc-489, Santa Cruz), anti-Id3 (1:100; C-20, sc-490, Santa Cruz), and anti-cardiac troponin T antibody (1:50; CT3, DSHB) antibodies were used. DAPI served as a counterstain. To immunostain C2C12 cells, anti-fast MyHC antibody (1:50; F59, DSHB) served as first antibody, followed by Alexa 594 (1:400; Molecular Probes) as second antibody. Nuclei were stained with DAPI. Whole cell extracts were prepared for western blotting. Rabbit polyclonal antisera for mouse RP58 (which recognizes the TVRDWTLEDSSQEC epitope) was obtained from Protein Purity, Ltd. (Japan).

Cell-Based HTS

We arrayed 6049 different expression vectors from the MGC (Mammalian Gene Collection) human cDNA expression vector library plus pcDNA3.1 (+) as a negative control on 384-well plates using 50 ng plasmid per well. High-throughput transfection assays were undertaken by incubation with 20 μl OPTI-MEM containing 0.1 μl of Lipofectamine 2000 and 20 ng of the pGL4.12-RP58-3.4k reporter vector for 20 min. Then we added 5×10^3 of 293T cells in 40 μl GM to each well and cultured for 48 hr. Luciferase activity was measured using the Steady-Glo luciferase assay system (Promega).

Luciferase Assay

Cells in 48-well plates at 50% confluence were transfected using FugeneHD (Roche). A firefly luciferase reporter gene construct (50 ng), an effector gene construct (50 ng), and 5 ng of pGL4.74 *Renilla* luciferase construct for normalization (Promega) were cotransfected per well. Cell extracts were prepared 36–48 hr after transfection and luciferase activity measured using the Dual-Luciferase Reporter Assay System (Promega).

Microarray Analysis

Sample RNAs were obtained from C2C12 cells stably expressing RP58-shRNA or control-shRNA cells, and from C2C12 cells cultured either in GM or in DM for 0, 2, and 4 days. Five micrograms of RNA was reverse transcribed using SuperScript II and a second strand cDNA was synthesized. Biotinylated antisense cRNAs were amplified and transcribed using the BioArray RNA Amplification and Labeling system (Enzo Life Science, NY, USA). Finally, 10 μg of cRNAs were hydrolyzed and hybridized to the GeneChip (R) Mouse Genome 430 2.0 array (Affymetrix). Microarray data were summarized using the Robust Multichip Average (RMA) method, and statistical analysis was performed using NIA Array Analysis (http://lgusun.grc.nia.nih.gov/ANOVA/; Chapman et al., 2005; Sharov et al., 2005). Upregulated genes were defined as showing a signal intensity elevated more than 1.5-fold compared with control cells. To identify genes downregulated in C2C12 myogenesis, principal component analysis (PCA) was performed and downregulated genes were identified. Microarray data are deposited in the Gene Expression Omnibus (GEO) under accession number GSE12993.

ChIP Assay

C2C12 cells infected with Flag-RP58-expressing adenovirus were cultured in DM for 2 days. Cells were crosslinked with 1% formaldehyde for 10 min and quenched with 0.125 M glycine for 5 min. Cells were washed with cell lysis buffer (5 mM PIPES [pH 8.0]; 85 mM KCl; 0.5% NP-40) and resuspended in nuclear lysis buffer (50 mM Tris-HCl [pH 8.1]; 10 mM EDTA; 1% SDS). Chromatin was sheared to approximately 300–500 bp by sonication and diluted 5 times with ChIP dilution buffer (16.7 mM Tris-HCl [pH 8.1]; 167 mM NaCl; 1.2 mM EDTA; 0.01% SDS; 1.1% Triton X-100). The chromatin solution was incubated with 2 μg anti-Flag-M2 (SIGMA) antibody or normal mouse IgG (Santa Cruz) and Dynabeads Protein G (Invitrogen) at 4°C. Beads were washed with ChIP wash buffer (50 mM HEPES-KOH [pH 7.0]; 0.5 M LiCl; 1 mM EDTA; 0.7% sodium deoxycholate; 1% NP-40) 3 times and once with TE buffer (10 mM Tris-HCl [pH 8.0]; 1 mM EDTA), and immune-complexes were eluted from beads with ChIP elution buffer (50 mM Tris-HCl [pH 8.0]; 10 mM EDTA; 1% SDS) at 65°C. Eluates were additionally incubated at 65°C to reverse crosslinking and then incubated with 0.5 mg/ml proteinase K at 55°C. DNA was purified by phenol-chloroform extraction and ethanol precipitation. In ChIP of MyoD or acetyl-histone 3, ChIP assay was performed with C2C12 cells cultured in GM until fully confluent or with cells incubated in DM for 2 days after reaching full confluence, using a SimpleChIP Enzymatic Chromatin IP Kit (Cell Signaling), according to the manufacturer's instructions. Protein-DNA complexes were precipitated with 2 μg of anti-MyoD antibody (sc-760; Santa Cruz), anti-acetyl-histone 3 antibody (06-598; Millipore), or normal rabbit IgG (Santa Cruz). Aliquots and whole-cell extracts (serving as input samples) were analyzed by PCR or quantitative real-time PCR amplification with the following primer pairs: (Id2-Forward) 5′-CGCGGGC GAGTCTCAAGGTC-3′, (Id2-Reverse) 5′-CAGGGATCACTCGGGGGGTC-3′; (Id3-Forward) 5′-CACGCATCCCTGTGTGAACG-3′, (Id3-Reverse) 5′-GAGGA ATCCGCTCCTTTGCC-3′; (RP58-E1-Forward) 5′-CTGGTGGCAGGAGTGTA GAG-3′, (RP58-E1-Reverse) 5′-CCGCACACACTAACTCCCTG-3′; (RP58-E2-Forward) 5′-GGCCAGACAGCTGTAATCGC-3′, (RP58-E2-Reverse) 5′-CAGA GGGACGAAGAAGGAAGC-3′.

MyoD-Dependent Myogenic Conversion of 10T1/2 Fibroblasts

10T1/2 fibroblasts were generated from wild-type and RP58 null mouse embryonic fibroblasts (MEFs). Myogenesis assays were performed using these newly established fibroblasts by ectopic expression of adenoviral MyoD. The activation of the myogenic program in these cells was induced by low serum conditions (DM, supplemented with insulin) and was monitored by the formation of myotubes expressing muscle-specific genes, such as Ckm and MyHC. Rescue experiments were performed by downregulating endogenous Id2 and Id3, by transfection of specific siRNA (purchased from QIAGEN). For immunostaining of MyHC, MF20 antibody (DSHB) was used.

Knockout Mice Embryos

C57BL/6J-Pax3Sp/J mice were purchased from Jackson Laboratory (Bar Harbor, ME). Homozygous mice (*Pax3*$^{Sp/Sp}$) embryos were identified by appearance of spina bifida and by PCR genotyping. Myog (Myogenin) knockout$^{+/-}$ mice were kindly provided from Y. Nabeshima. Homozygous *Myog*$^{-/-}$ and *WT* mice were identified by PCR. All embryos were obtained by timed mating. The morning of the appearance of the vaginal plug was designated E0.5.

Statistical Analysis

The two-tailed independent Student's t test was used to calculate all *P* values. Asterisks in figures indicate differences with statistical significance as follows: *$p < 0.05$, **$p < 0.01$, and ***$p < 0.001$.

SUPPLEMENTAL DATA

Supplemental Data include nine figures and eleven tables and can be found with this article online at http://www.cell.com/developmental-cell/supplemental/S1534-5807(09)00433-X.

ACKNOWLEDGMENTS

We thank H. Naito, T. Suzuki, D. Kozaki, H. Ishitobi, M. Horiuchi, K.Sakuma, J. Hasegawa, and all other Asahara lab members for help with construction of EMBRYS; M. Asada, T. Watanabe, and T. Yoshitaka for construction and assistance with HTS; G. Lindman for assistance with vector construction; Y. Kawakami and J.C. Belmonte for technical advice; Y. Takahashi and K. Yanagisawa for help with bioinformatics information and construction of the webpage; N. Hashimoto for help with setting up microarray instruments; A. Miwa for help with collecting RP58 mutant embryos; Y. Nabeshima for sharing *Myog* mutant mice; and T. Tanaka, S. Hiraoka, and G. Lindman for critical reading of the manuscript and discussion. Y. Ito and H. Asahara are associate scientists of Tokyo Medical & Dental University. This project was supported by Grants from the Genome Network Project (MEXT) and partially from SORST (JST), Grants from the Ministry of Health, Labour and Welfare, Grants-in Aid for Scientific Research (MEXT), and Grant ID 05-24 from the National Institute of Biomedical Innovation. P.L.P is an associate scientist of Telethon Dulbecco Institute and of Sanford Children's Health Center and was partially supported by AIRC and NIAMS (RO1AR052779).

Received: March 2, 2009
Revised: August 20, 2009
Accepted: October 6, 2009
Published: December 14, 2009

REFERENCES

Aoki, K., Meng, G., Suzuki, K., Takashi, T., Kameoka, Y., Nakahara, K., Ishida, R., and Kasai, M. (1998). RP58 associates with condensed chromatin and mediates a sequence-specific transcriptional repression. J. Biol. Chem. *273*, 26698–26704.

Arnold, H.H., and Braun, T. (1996). Targeted inactivation of myogenic factor genes reveals their role during mouse myogenesis: a review. Int. J. Dev. Biol. *40*, 345–353.

Benezra, R., Davis, R.L., Lockshon, D., Turner, D.L., and Weintraub, H. (1990). The protein Id: a negative regulator of helix-loop-helix DNA binding proteins. Cell *61*, 49–59.

Blackwell, T.K., and Weintraub, H. (1990). Differences and similarities in DNA-binding preferences of MyoD and E2A protein complexes revealed by binding site selection. Science *250*, 1104–1110.

Blackwell, T.K., Kretzner, L., Blackwood, E.M., Eisenman, R.N., and Weintraub, H. (1990). Sequence-specific DNA binding by the c-Myc protein. Science *250*, 1149–1151.

Blais, A., Tsikitis, M., Acosta-Alvear, D., Sharan, R., Kluger, Y., and Dynlacht, B.D. (2005). An initial blueprint for myogenic differentiation. Genes Dev. *19*, 553–569.

Blau, H.M., Chiu, C.P., and Webster, C. (1983). Cytoplasmic activation of human nuclear genes in stable heterocaryons. Cell *32*, 1171–1180.

Bober, E., Franz, T., Arnold, H.H., Gruss, P., and Tremblay, P. (1994). Pax-3 is required for the development of limb muscles: a possible role for the migration of dermomyotomal muscle progenitor cells. Development *120*, 603–612.

Braun, T., Rudnicki, M.A., Arnold, H.H., and Jaenisch, R. (1992). Targeted inactivation of the muscle regulatory gene Myf-5 results in abnormal rib development and perinatal death. Cell *71*, 369–382.

Burke, A.C., Nelson, C.E., Morgan, B.A., and Tabin, C. (1995). Hox genes and the evolution of vertebrate axial morphology. Development *121*, 333–346.

Cao, Y., Kumar, R.M., Penn, B.H., Berkes, C.A., Kooperberg, C., Boyer, L.A., Young, R.A., and Tapscott, S.J. (2006). Global and gene-specific analyses show distinct roles for Myod and Myog at a common set of promoters. EMBO J. *25*, 502–511.

Chapman, S., Schenk, P., Kazan, K., and Manners, J. (2002). Using biplots to interpret gene expression patterns in plants. Bioinformatics *18*, 202–204.

Chen, B., Han, B.H., Sun, X.H., and Lim, R.W. (1997). Inhibition of muscle-specific gene expression by Id3: requirement of the C-terminal region of the protein for stable expression and function. Nucleic Acids Res. *25*, 423–430.

Daston, G., Lamar, E., Olivier, M., and Goulding, M. (1996). Pax-3 is necessary for migration but not differentiation of limb muscle precursors in the mouse. Development *122*, 1017–1027.

Di Padova, M., Caretti, G., Zhao, P., Hoffman, E.P., and Sartorelli, V. (2007). MyoD acetylation influences temporal patterns of skeletal muscle gene expression. J. Biol. Chem. *282*, 37650–37659.

Frazer, K.A., Pachter, L., Poliakov, A., Rubin, E.M., and Dubchak, I. (2004). VISTA: computational tools for comparative genomics. Nucleic Acids Res. *32*, W273–W279.

Fuks, F., Burgers, W.A., Godin, N., Kasai, M., and Kouzarides, T. (2001). Dnmt3a binds deacetylases and is recruited by a sequence-specific repressor to silence transcription. EMBO J. *20*, 2536–2544.

Gray, P.A., Fu, H., Luo, P., Zhao, Q., Yu, J., Ferrari, A., Tenzen, T., Yuk, D.I., Tsung, E.F., Cai, Z., et al. (2004). Mouse brain organization revealed through direct genome-scale TF expression analysis. Science *306*, 2255–2257.

Guasconi, V., and Puri, P.L. (2009). Chromatin: the interface between extrinsic cues and the epigenetic regulation of muscle regeneration. Trends Cell Biol. *19*, 286–294.

Hasty, P., Bradley, A., Morris, J.H., Edmondson, D.G., Venuti, J.M., Olson, E.N., and Klein, W.H. (1993). Muscle deficiency and neonatal death in mice with a targeted mutation in the myogenin gene. Nature *364*, 501–506.

Iourgenko, V., Zhang, W., Mickanin, C., Daly, I., Jiang, C., Hexham, J.M., Orth, A.P., Miraglia, L., Meltzer, J., Garza, D., et al. (2003). Identification of a family of cAMP response element-binding protein coactivators by genome-scale functional analysis in mammalian cells. Proc. Natl. Acad. Sci. USA *100*, 12147–12152.

Jen, Y., Weintraub, H., and Benezra, R. (1992). Overexpression of Id protein inhibits the muscle differentiation program: in vivo association of Id with E2A proteins. Genes Dev. *6*, 1466–1479.

Jessell, T.M. (2000). Neuronal specification in the spinal cord: inductive signals and transcriptional codes. Nat. Rev. Genet. *1*, 20–29.

Kanamori, M., Konno, H., Osato, N., Kawai, J., Hayashizaki, Y., and Suzuki, H. (2004). A genome-wide and nonredundant mouse transcription factor database. Biochem. Biophys. Res. Commun. *322*, 787–793.

Kassar-Duchossoy, L., Gayraud-Morel, B., Gomes, D., Rocancourt, D., Buckingham, M., Shinin, V., and Tajbakhsh, S. (2004). Mrf4 determines skeletal muscle identity in Myf5:Myod double-mutant mice. Nature *431*, 466–471.

Kawakami, Y., Rodriguez-Leon, J., Koth, C.M., Buscher, D., Itoh, T., Raya, A., Ng, J.K., Esteban, C.R., Takahashi, S., Henrique, D., et al. (2003). MKP3 mediates the cellular response to FGF8 signalling in the vertebrate limb. Nat. Cell Biol. *5*, 513–519.

Kent, W.J. (2002). BLAT–the BLAST-like alignment tool. Genome Res. *12*, 656–664.

Kurabayashi, M., Jeyaseelan, R., and Kedes, L. (1994). Doxorubicin represses the function of the myogenic helix-loop-helix transcription factor MyoD. Involvement of Id gene induction. J. Biol. Chem. *269*, 6031–6039.

Langlands, K., Yin, X., Anand, G., and Prochownik, E.V. (1997). Differential interactions of Id proteins with basic-helix-loop-helix transcription factors. J. Biol. Chem. *272*, 19785–19793.

Lein, E.S., Hawrylycz, M.J., Ao, N., Ayres, M., Bensinger, A., Bernard, A., Boe, A.F., Boguski, M.S., Brockway, K.S., Byrnes, E.J., et al. (2007). Genome-wide atlas of gene expression in the adult mouse brain. Nature *445*, 168–176.

Mariani, F.V., and Martin, G.R. (2003). Deciphering skeletal patterning: clues from the limb. Nature *423*, 319–325.

McKinsey, T.A., Zhang, C.L., and Olson, E.N. (2001). Control of muscle development by dueling HATs and HDACs. Curr. Opin. Genet. Dev. *11*, 497–504.

Melnikova, I.N., and Christy, B.A. (1996). Muscle cell differentiation is inhibited by the helix-loop-helix protein Id3. Cell Growth Differ. *7*, 1067–1079.

Melnikova, I.N., Bounpheng, M., Schatteman, G.C., Gilliam, D., and Christy, B.A. (1999). Differential biological activities of mammalian Id proteins in muscle cells. Exp. Cell Res. *247*, 94–104.

Murre, C., McCaw, P.S., and Baltimore, D. (1989). A new DNA binding and dimerization motif in immunoglobulin enhancer binding, daughterless, MyoD, and myc proteins. Cell *56*, 777–783.

Nabeshima, Y., Hanaoka, K., Hayasaka, M., Esumi, E., Li, S., and Nonaka, I. (1993). Myogenin gene disruption results in perinatal lethality because of severe muscle defect. Nature *364*, 532–535.

Neuhold, L.A., and Wold, B. (1993). HLH forced dimers: tethering MyoD to E47 generates a dominant positive myogenic factor insulated from negative regulation by Id. Cell *74*, 1033–1042.

Ohtaka-Maruyama, C., Miwa, A., Kawano, H., Kasai, M., and Okado, H. (2007). Spatial and temporal expression of RP58, a novel zinc finger transcriptional repressor, in mouse brain. J. Comp. Neurol. *502*, 1098–1108.

Okado, H., Ohtaka-Maruyama, C., Sugitani, Y., Fukuda, Y., Ishida, R., Hirai, S., Miwa, A., Takahashi, A., Aoki, K., Mochida, K., et al. (2009). The transcriptional repressor RP58 is crucial for cell-division patterning and neuronal survival in the developing cortex. Dev. Biol. *331*, 140–151.

Penn, B.H., Bergstrom, D.A., Dilworth, F.J., Bengal, E., and Tapscott, S.J. (2004). A MyoD-generated feed-forward circuit temporally patterns gene expression during skeletal muscle differentiation. Genes Dev. *18*, 2348–2353.

Puri, P.L., and Sartorelli, V. (2000). Regulation of muscle regulatory factors by DNA-binding, interacting proteins, and post-transcriptional modifications. J. Cell. Physiol. *185*, 155–173.

Puri, P.L., Sartorelli, V., Yang, X.J., Hamamori, Y., Ogryzko, V.V., Howard, B.H., Kedes, L., Wang, J.Y., Graessmann, A., Nakatani, Y., and Levrero, M. (1997). Differential roles of p300 and PCAF acetyltransferases in muscle differentiation. Mol. Cell *1*, 35–45.

Riddle, R.D., Johnson, R.L., Laufer, E., and Tabin, C. (1993). Sonic hedgehog mediates the polarizing activity of the ZPA. Cell *75*, 1401–1416.

Rudnicki, M.A., Braun, T., Hinuma, S., and Jaenisch, R. (1992). Inactivation of MyoD in mice leads to up-regulation of the myogenic HLH gene Myf-5 and results in apparently normal muscle development. Cell *71*, 383–390.

Sartorelli, V., Puri, P.L., Hamamori, Y., Ogryzko, V., Chung, G., Nakatani, Y., Wang, J.Y., and Kedes, L. (1999). Acetylation of MyoD directed by PCAF is necessary for the execution of the muscle program. Mol. Cell *4*, 725–734.

Saunders, J.W., Jr. (1948). The proximo-distal sequence of origin of the parts of the chick wing and the role of the ectoderm. J. Exp. Zool. *108*, 363–403.

Seo, S., Lim, J.W., Yellajoshyula, D., Chang, L.W., and Kroll, K.L. (2007). Neurogenin and NeuroD direct transcriptional targets and their regulatory enhancers. EMBO J. *26*, 5093–5108.

Sharov, A.A., Dudekula, D.B., and Ko, M.S. (2005). A web-based tool for principal component and significance analysis of microarray data. Bioinformatics *21*, 2548–2549.

Takahashi, K., and Yamanaka, S. (2006). Induction of pluripotent stem cells from mouse embryonic and adult fibroblast cultures by defined factors. Cell *126*, 663–676.

Thomas, P.D., Campbell, M.J., Kejariwal, A., Mi, H., Karlak, B., Daverman, R., Diemer, K., Muruganujan, A., and Narechania, A. (2003). PANTHER: a library of protein families and subfamilies indexed by function. Genome Res. *13*, 2129–2141.

Weintraub, H., Tapscott, S.J., Davis, R.L., Thayer, M.J., Adam, M.A., Lassar, A.B., and Miller, A.D. (1989). Activation of muscle-specific genes in pigment, nerve, fat, liver, and fibroblast cell lines by forced expression of MyoD. Proc. Natl. Acad. Sci. USA *86*, 5434–5438.

Williams, B.A., and Ordahl, C.P. (1994). Pax-3 expression in segmental mesoderm marks early stages in myogenic cell specification. Development *120*, 785–796.

Wolpert, L. (1969). Positional information and the spatial pattern of cellular differentiation. J. Theor. Biol. *25*, 1–47.

Wu, J., and Lim, R.W. (2005). Regulation of inhibitor of differentiation gene 3 (Id3) expression by Sp2-motif binding factor in myogenic C2C12 cells: downregulation of DNA binding activity following skeletal muscle differentiation. Biochim. Biophys. Acta *1731*, 13–22.

Yaffe, D., and Saxel, O. (1977). Serial passaging and differentiation of myogenic cells isolated from dystrophic mouse muscle. Nature *270*, 725–727.

Yokoyama, S., Hashimoto, M., Shimizu, H., Ueno-Kudoh, H., Uchibe, K., Kimura, I., and Asahara, H. (2008). Dynamic gene expression of Lin-28 during embryonic development in mouse and chicken. Gene Expr. Patterns *8*, 155–160.

Zhang, W., Behringer, R.R., and Olson, E.N. (1995). Inactivation of the myogenic bHLH gene MRF4 results in up-regulation of myogenin and rib anomalies. Genes Dev. *9*, 1388–1399.

Zhou, Q., Brown, J., Kanarek, A., Rajagopal, J., and Melton, D.A. (2008). In vivo reprogramming of adult pancreatic exocrine cells to β-cells. Nature *455*, 627–632.

ARTHRITIS & RHEUMATISM
Vol. 60, No. 9, September 2009, pp 2723–2730
DOI 10.1002/art.24745

MicroRNA-140 Is Expressed in Differentiated Human Articular Chondrocytes and Modulates Interleukin-1 Responses

Shigeru Miyaki,[1] Tomoyuki Nakasa,[2] Shuhei Otsuki,[1] Shawn P. Grogan,[1] Reiji Higashiyama,[1] Atsushi Inoue,[2] Yoshio Kato,[3] Tempei Sato,[2] Martin K. Lotz,[1] and Hiroshi Asahara[4]

Objective. **MicroRNA (miRNA) are a class of noncoding small RNAs that act as negative regulators of gene expression. MiRNA exhibit tissue-specific expression patterns, and changes in their expression may contribute to pathogenesis. The objectives of this study were to identify miRNA expressed in articular chondrocytes, to determine changes in osteoarthritic (OA) cartilage, and to address the function of miRNA-140 (miR-140).**

Methods. **To identify miRNA specifically expressed in chondrocytes, we performed gene expression profiling using miRNA microarrays and quantitative polymerase chain reaction with human articular chondrocytes compared with human mesenchymal stem cells (MSCs). The expression pattern of miR-140 was monitored during chondrogenic differentiation of human MSCs in pellet cultures and in human articular cartilage from normal and OA knee joints. We tested the effects of interleukin-1β (IL-1β) on miR-140 expression. Double-stranded miR-140 (ds–miR-140) was transfected into chondrocytes to analyze changes in the expression of genes associated with OA.**

Results. **Microarray analysis showed that miR-140 had the largest difference in expression between chondrocytes and MSCs. During chondrogenesis, miR-140 expression in MSC cultures increased in parallel with the expression of *SOX9* and *COL2A1*. Normal human articular cartilage expressed miR-140, and this expression was significantly reduced in OA tissue. In vitro treatment of chondrocytes with IL-1β suppressed miR-140 expression. Transfection of chondrocytes with ds–miR-140 down-regulated IL-1β–induced *ADAMTS5* expression and rescued the IL-1β–dependent repression of *AGGRECAN* gene expression.**

Conclusion. **This study shows that miR-140 has a chondrocyte differentiation–related expression pattern. The reduction in miR-140 expression in OA cartilage and in response to IL-1β may contribute to the abnormal gene expression pattern characteristic of OA.**

Osteoarthritis (OA) is a chronic and highly prevalent degenerative joint disease. Approximately 40 million Americans are currently affected, and this number is predicted to increase to 60 million within the next 20 years as a result of population aging and an increase in life expectancy (1,2). Current treatment is limited to pain management, and disease-modifying therapies are not available in the late phase of the disease process, at which point joint replacement surgery is often indicated. OA has been associated with age-related loss of the homeostatic balance between degradation and repair mechanisms. Cartilage cellularity in OA is reduced by chondrocyte death, and remaining chondrocytes are activated by cytokines and growth factors to a catabolic and abnormal differentiation that leads to degradation

Supported by the Sam and Rose Stein Endowment. Dr. Otsuki's work was supported by the Arthritis Foundation. Dr. Lotz's work was supported by NIH grants AG-033409 and AG-007996. Dr. Asahara's work was supported by NIH grants AR-050631 and AR-056120, Health and Labour Sciences Research grants, and Grants-in-Aid for Scientific Research (MEXT).

[1]Shigeru Miyaki, PhD, Shuhei Otsuki, MD, PhD, Shawn P. Grogan, PhD, Reiji Higashiyama, MD, PhD, Martin K. Lotz, MD: Scripps Research Institute, La Jolla, California; [2]Tomoyuki Nakasa, MD, PhD, Atsushi Inoue, PhD, Tempei Sato, MS: National Research Institute for Child Health and Development, Tokyo, Japan; [3]Yoshio Kato, PhD: Research Institute for Cell Engineering, National Institute of Advanced Industrial Science and Technology, Osaka, Japan; [4]Hiroshi Asahara, MD, PhD: Scripps Research Institute, La Jolla, California, and National Research Institute for Child Health and Development, Tokyo, Japan.

Address correspondence and reprint requests to Hiroshi Asahara, MD, PhD, Department of Molecular and Experimental Medicine, Scripps Research Institute, 10550 North Torrey Pines Road, La Jolla, CA 92037. E-mail: asahara@scripps.edu.

Submitted for publication December 22, 2008; accepted in revised form May 17, 2009.

of extracellular matrix (ECM) (3–6). Molecular mechanisms that govern articular chondrocyte differentiation during development and maintenance of articular cartilage are being characterized, and this has the potential to lead to new therapeutic interventions.

MicroRNA (miRNA) are a class of noncoding small RNAs that play roles in biologic processes as negative regulators of gene expression by promoting messenger RNA (mRNA) degradation and/or repressing translation through sequence-specific interactions with the 3′-untranslated regions of specific mRNA targets (7–10). Hundreds of miRNA have been found in various organisms, and many miRNA are evolutionarily conserved. Moreover, one-third of all mammalian mRNA seem to be under miRNA regulation, suggesting an essential role in regulating gene expression (11). Several miRNA exhibit a tissue- or developmental stage–specific expression pattern and have been associated with diseases such as cancer, heart disease, diabetes, and rheumatoid arthritis (12–16). Mice with limb- or cartilage-specific deletion of the miRNA processing enzyme Dicer showed a severe phenotype with reduced limb size but normal patterning (17,18). Because Dicer is indispensable for producing a functional, mature type of miRNA, this finding suggests that the presence of specific miRNA plays a critical role in skeletal development. Although Tuddenham et al showed cartilage-specific expression of miRNA-140 (miR-140) in mouse embryos (19), the role of tissue-specific miRNA in articular cartilage has not been reported.

We hypothesized that miRNA are novel regulators of cartilage homeostasis, and that changes in their expression and function play an important role in diseases affecting articular cartilage. The objectives of this study were to identify miRNA expressed in articular chondrocytes, to determine changes in OA cartilage, and to address the function of chondrocyte-specific miR-140.

MATERIALS AND METHODS

Human tissue samples, cell isolation, and culture. Human articular cartilage specimens were obtained from the knee joints of 8 normal donors (mean ± SD age 38.22 ± 5.31 years) and from 11 patients with OA (mean ± SD age 79.36 ± 9.72 years) who were undergoing total knee arthroplasty. Tissue collection was approved by the Scripps Human Subjects Committee. All samples were examined by Safranin O staining and graded according to a modified Mankin scale (20), with a score of <2 points being normal and a score of >5 representing OA. RNA was isolated from fresh-frozen cartilage by homogenizing the tissue in a freezer mill (Spex, Metuchen, NJ) and extracting the homogenate in TRIzol (Invitrogen, Carlsbad, CA). Human chondrocytes were isolated and cultured as described previously (21). Experiments with chondrocytes were performed in passages 1–2. Human bone marrow–derived mesenchymal stem cells (MSCs) were isolated from iliac crest bone marrow obtained from normal adult donors (with the approval of the Human Subjects Committee) and cultured as described previously (21,22). Experiments with MSCs were performed in passages 3–6.

Microarray analysis. Small RNAs of <200 nucleotides in length were extracted from MSCs and chondrocytes with the mirVana miRNA Isolation Kit (Ambion, Austin, TX) according to the manufacturer's protocol. Purified RNA was then labeled with Cy3 or Cy5, using the mirVana miRNA Labeling Kit. Briefly, RNA was subjected to a tailing reaction with amine-modified nucleotide triphosphates by poly(A) polymerase, followed by amide formation using Cy dye ester. Labeled RNAs were hybridized on slides, on which oligonucleotides against human miRNA had been arrayed (Hokkaido System Science, Hokkaido, Japan), and detected by a scanner (Agilent, Santa Clara, CA).

Chondrogenesis in human MSCs. Human bone marrow MSCs were used to prepare pellets (5.0×10^5 cells/pellet) by centrifuging the cells at 500*g* in 15-ml conical polypropylene tubes and culturing them in chondrogenic medium (Lonza, Walkersville, MD) supplemented with bone morphogeneic protein 2 (500 ng/ml) and transforming growth factor β3 (10 ng/ml). Medium was changed every 2–3 days. To monitor miR-140 throughout chondrogenesis, MSCs were processed for RNA isolation on day 7 and day 14. Chondrogenesis was monitored via *SOX9*, *AGGRECAN*, and *COL2A1* expression and Safranin O staining.

Treatment with interleukin-1β (IL-1β). Chondrocytes were maintained in 12-well plates containing Dulbecco's modified Eagle's medium plus 10% calf serum and 1% penicillin/streptomycin. Following treatment with recombinant human IL-1β (5 ng/ml; PeproTech, Rocky Hill, NJ), cells were washed with cold phosphate buffered saline, and total RNA was isolated with TRIzol reagent. Quantitative polymerase chain reaction (PCR) was performed with the TaqMan MicroRNA Assay Kit (Applied Biosystems, Foster City, CA) for mature

Table 1. MicroRNA expression in human articular chondrocytes and MSCs*

MicroRNA	Ratio, chondrocytes:MSCs	Chondrocytes	MSCs
miR-140	2.12	540.89	254.37
miR-197	1.88	5,395.03	2,869.38
miR-148	1.78	644.35	361.58
miR-328	1.70	2,768.41	1,632.95
miR-27b	1.63	6,092.21	3,746.00
miR-16	1.59	4,398.78	2,764.09
miR-222	1.55	6,349.65	4,087.27
miR-15b	1.55	668.29	430.56
miR-505	1.54	1,967.68	1,273.77
miR-23b	1.52	8,114.26	5,334.24

* RNA was isolated from articular chondrocytes and mesenchymal stem cells (MSCs) for microarray analysis of microRNA. Differentially expressed microRNA (at least 1.5-fold difference) are shown as the ratio of chondrocytes to MSCs. Values for chondrocytes and human MSCs are the raw signal intensities.

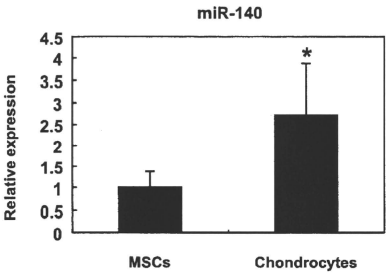

Figure 1. Expression of microRNA-140 (miR-140) in articular chondrocytes and human mesenchymal stem cells (MSCs). Array data for miR-140 were validated by quantitative polymerase chain reaction on MSCs (3 different preparations from 3 different donors) and articular chondrocytes (8 different preparations from 8 different donors). MiR-140 expression was significantly higher in chondrocytes compared with MSCs. Bars show the mean and SEM fold difference in relative expression. * = $P = 0.015$.

miR-140 or with the TaqMan Gene Expression Assay for chondrogenic markers *MMP13* and *ADAMTS5*.

Transfection of double-stranded miR-140 (ds–miR-140) into human articular chondrocytes. Double-stranded RNA (dsRNA) oligonucleotides representing mature sequences that mimic endogenous miR-140 were transfected into human chondrocytes at 80–90% confluence (4-n*M* concentration) with Lipofectamine 2000 (Invitrogen) according to the manufacturer's instructions. Synthesized RNA oligonucleotides 5′-CAGUGGUUUUACCCUAUGGUAG-3′ and 5′-ACCACAGGGUAGAACCACGGAC-3′ were annealed to obtain ds–miR-140. Silencer Negative Control #1 small interfering RNA (Ambion) at the same concentration as the specific ds–miR-140 was used in each experiment.

Real-time quantitative PCR. Total RNA was isolated from cartilage tissues, monolayer cultures, or pellet cultures using TRIzol. Real-time quantitative PCR for miRNA was performed using the TaqMan MicroRNA Reverse Transcription Kit (Applied Biosystems) according to the manufacturer's protocol. Complementary DNA was produced using Ready-to-Go You-Prime First-Strand Beads (GE Healthcare, Chalfont, UK) with total RNA (1 μg) and oligo$(dT)_{18}$ primers. Real-time quantitative PCR was performed using TaqMan Gene Expression Assay probes for *COL2A1* (Hs00164004_m1),

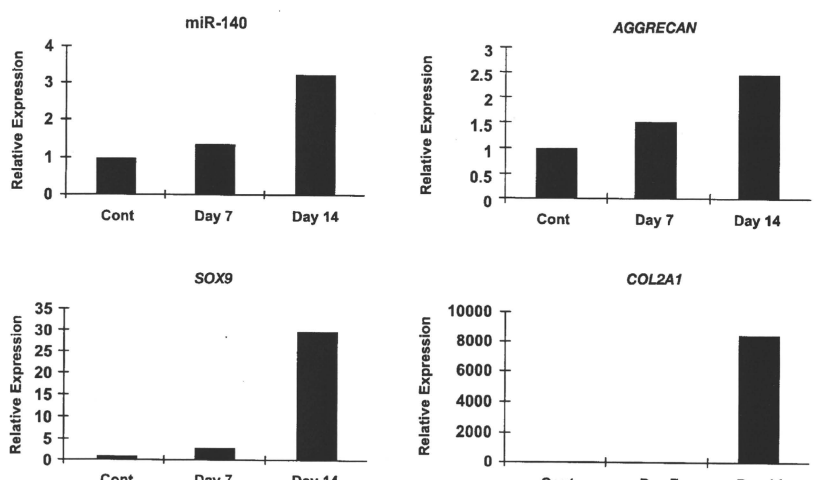

Figure 2. Changes in miR-140 expression during chondrogenesis. RNA was isolated from undifferentiated MSCs (controls [Cont]) and from MSC pellet cultures in chondrogenesis medium on day 7 and day 14. The expression of miR-140, *AGGRECAN*, *SOX9*, and *COL2A1* was analyzed by quantitative polymerase chain reaction. The expression of miR-140 increased during chondrogenesis, along with increased expression of *SOX9*, *AGGRECAN*, and *COL2A1*. Results are shown as the relative expression, where expression in undifferentiated MSCs is defined as 1. See Figure 1 for other definitions.

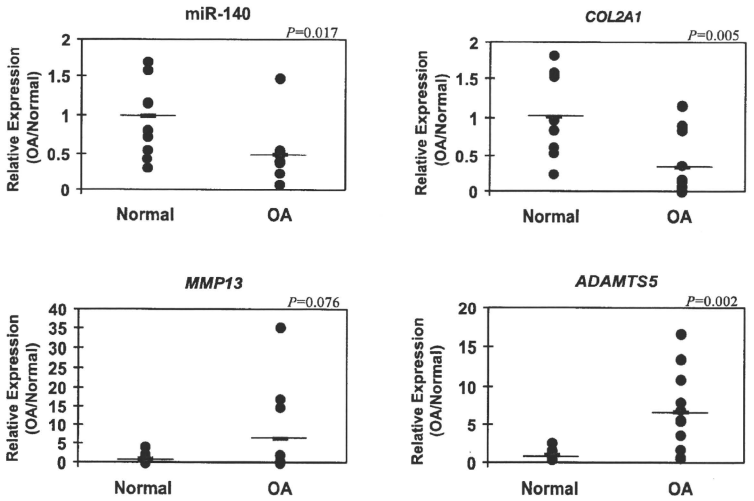

Figure 3. MicroRNA-140 (miR-140) expression in normal and osteoarthritis (OA) articular cartilage. Full-thickness cartilage specimens were collected from normal (n = 8) and OA (n = 11) knee joints for RNA isolation. The expression of miR-140, *COL2A1*, *ADAMTS5*, and *SOX9* was determined by quantitative polymerase chain reaction. The expression of miR-140 and *COL2A1* was significantly decreased, and the expression of *ADAMTS5* was significantly increased in OA cartilage compared with normal cartilage. Bars show the mean.

AGGRECAN (Hs00202971_m1), *ADAMTS5* (Hs00199841_m1), *MMP13* (Hs00233992_m1), and *GAPDH* (Hs99999905_m1) (Applied Biosystems). The U18 and GAPDH genes were used as an internal control to normalize differences in each sample. The expression levels for each gene were assessed relative to the expression of U18 or GAPDH.

Statistical analysis. Statistically significant differences between 2 groups were determined with *t*-tests. The results are reported as the mean ± SEM. *P* values less than 0.05 were considered significant.

RESULTS

MicroRNA-140 expression in articular chondrocytes and MSCs. Chondrogenic differentiation of MSCs involves dynamic changes in various gene expression patterns such as induced expression of chondrocyte-specific genes, including *SOX9* and *COL2A1*. In order to screen miRNA specifically expressed in chondrocytes, we performed gene expression profiling using miRNA microarrays comparing primary chondrocytes from articular cartilage with MSCs. Several miRNA were more abundant in primary articular chondrocytes than in undifferentiated MSCs. The largest difference was observed for miR-140 (Table 1). The high expression of miR-140 in chondrocytes compared with MSCs was confirmed by quantitative PCR (Figure 1).

Expression of miR-140 during chondrogenesis of MSCs. To examine the dynamic expression pattern of miR-140 during in vitro chondrogenesis, we performed a TaqMan quantitative PCR assay to analyze expression patterns of miR-140. Pellets of MSCs were strongly stained by Safranin O after chondrogenesis induction for 14 days (data not shown). In this model, miR-140 expression gradually increased during chondrogenesis in parallel with expression of *SOX9*, *AGGRECAN*, and *COL2A1* (Figure 2). These data indicate that the expres-

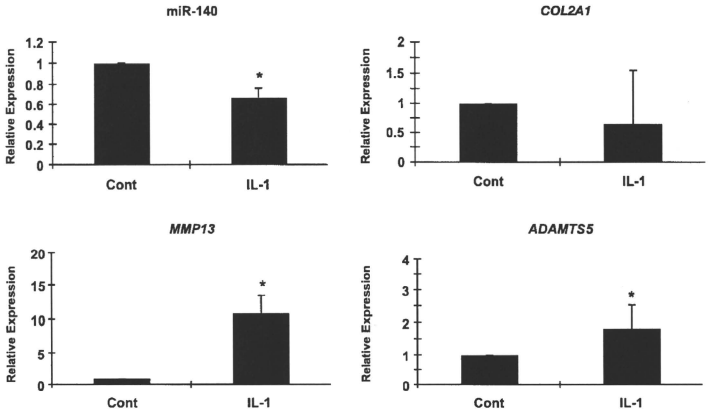

Figure 4. In vitro suppression of microRNA-140 (miR-140) by interleukin-1β (IL-1β). Articular chondrocytes (8 different preparations from 8 different donors) were treated with IL-1β (5 ng/ml) for 5 hours. The expression of miR-140, *COL2A1*, *MMP13*, and *ADAMTS5* was analyzed by quantitative polymerase chain reaction. IL-1β stimulation significantly decreased miR-140 expression and increased *MMP13* and *ADAMTS5* expression. *COL2A1* expression did not change significantly. Bars show the mean and SEM fold difference in relative expression. * = $P < 0.05$ versus control (Cont).

sion of miR-140 increases during chondrocytic differentiation of MSCs, and this is consistent with its high expression in chondrocytes.

Expression of miR-140 in normal and OA cartilage. In OA pathogenesis, several chondrocyte-specific genes, including *COL2A1* and *SOX9*, are down-regulated (23). In contrast, cartilage-degrading enzymes, including ADAMTS-5 and matrix metalloproteinase 13 (MMP-13), are up-regulated (24–26). To examine changes in miR-140 expression in OA articular cartilage, quantitative PCR of miR-140 together with OA-related marker genes was performed on 19 samples prepared from human knee articular cartilage (8 normal and 11 OA). As expected, the expression of *ADAMTS5* was significantly increased in OA cartilage, while the expression of *COL2A1* was significantly lower than that in normal cartilage (Figure 3). MiR-140 expression in articular cartilage from donors with OA (65–93 years old; Mankin score 5–10) was significantly lower than that in normal cartilage (obtained from individuals 30–44 years old; Mankin score 0–2) (Figure 3). These data demonstrate abnormally reduced miR-140 expression in OA cartilage and appear to correlate with increased *ADAMTS5* expression and reduced *COL2A1* expression in the same samples.

Effect of IL-1β on miR-140 expression in articular chondrocytes. IL-1β is one of the critical mediators of OA, and IL-1β stimulation of chondrocytes causes gene expression patterns similar to those of OA cartilage (27,28). To analyze the effects of IL-1β on the expression of miR-140 in articular chondrocytes, we performed quantitative PCR for miR-140 and *COL2A1*, *AGGRECAN*, *MMP13*, and *ADAMTS5*. In response to IL-1β stimulation, the expression of miR-140 was markedly decreased, while the expression of *MMP13* and *ADAMTS5* was significantly increased (Figure 4). Under the same experimental conditions, the expression of *COL2A1* did not change significantly. Taken together, these results show reduced miR-140 expression in the context of IL-1β–induced OA-like changes in chondrocyte gene expression.

Modulation of *ADAMTS5* and aggrecan expression in articular chondrocytes by miR-140. To investigate the function of miR-140 in chondrocytes, we examined whether expression of the OA-related genes *ADAMTS5*, *MMP13*, *COL2A1*, and *AGGRECAN* can be

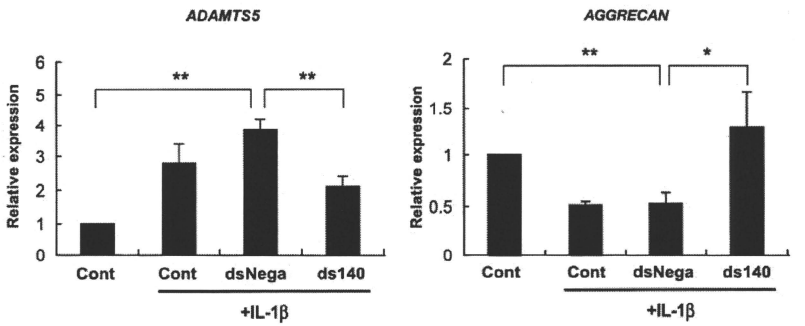

Figure 5. *ADAMTS5* and *AGGRECAN* expression by double-stranded microRNA-140 (ds–miR-140; ds140) in articular chondrocytes. Articular chondrocytes (n = 3) were transfected with ds–miR-140. The expression of *ADAMTS5* and *AGGRECAN* was analyzed by quantitative polymerase chain reaction. *ADAMTS5* expression was significantly reduced by ds–miR-140 with interleukin-1β (IL-1β) stimulation, and *AGGRECAN* expression was significantly increased by ds–miR-140 with IL-1β stimulation. Bars show the mean and SEM fold difference relative to control (Cont). dsNega = negative control of ds–miR-140 with nonspecific sequence. * = $P < 0.05$; ** = $P < 0.01$.

regulated by miR-140, when chondrocytes were stimulated with IL-1β with and without transfection of ds–miR-140. *ADAMTS5* expression with IL-1β stimulation was significantly reduced by ds–miR-140, and, conversely, *AGGRECAN* expression with IL-1β stimulation was significantly increased by ds–miR-140 (Figure 5). In the absence of IL-1β, the nonspecific dsRNA (dsNega) did not change the basal levels of *AGGRECAN*, and we observed an increase in *ADAMTS5* mRNA with ds–miR-140 as well as with dsNega. The expression of *MMP13* and *COL2A1* was not significantly changed by ds–miR-140 (data not shown). These results demonstrated that miR-140 regulates genes encoding ADAMTS-5 and aggrecan, suggesting that miR-140 plays an important role in regulating the balance between ECM formation and degradation.

DISCUSSION

This study is the first to identify miRNA that are expressed in a differentiation-dependent pattern in MSCs and articular chondrocytes. We also show changes in expression of the selected miR-140 in OA cartilage and in response to IL-1β stimulation. Moreover, we demonstrate that ADAMTS-5, a critical proteinase in OA pathogenesis (29–31), is regulated by miR-140.

Previous studies using systematic whole-mount in situ hybridization analysis for miRNA in zebrafish revealed that many miRNA are expressed in a tissue-specific pattern (32). From this database annotation, miR-140 was the only miRNA with a cartilage-specific expression pattern. Zebrafish embryos injected with ds–miR-140 had a profound facial phenotype, including cranial hemorrhaging and a hypoplastic roof of the mouth (33). Our miRNA array screen detected several miRNA that show large differences in expression in articular chondrocytes versus MSCs, including miR-140, which showed the largest expression difference between the 2 cell types. We also showed that during chondrogenesis, miR-140 expression increased in differentiated human MSCs compared with undifferentiated MSCs in parallel with expression of *SOX9*, *AGGRECAN*, and *COL2A1*. These findings suggest that miR-140 is a marker and possibly a regulator of chondrocyte differentiation.

The unique differentiation-related expression pattern of miR-140 is highlighted by our findings for miR-146, which is also expressed in chondrocytes. In contrast to miR-140, miR-146 has a broader tissue distribution, its expression is increased in response to IL-1 stimulation, it is up-regulated in OA (34), and it does not show changes related to chondrocyte differentiation (data not shown).

The ability of chondrocytes to remodel and repair cartilage ECM declines with aging, and in OA this is